AMERICAN SOCIETY FOR MICROBIOLOGY | Molecular and Cellular Biology®

RESEARCH ARTICLE

Peroxiredoxin 5 Inhibits Glutamate-Induced Neuronal Cell Death through the Regulation of Calcineurin-Dependent Mitochondrial Dynamics in HT22 Cells

Mi Hye Kim,[a,b] Hong Jun Lee,[c,d,e] Sang-Rae Lee,[f] Hyun-Shik Lee,[a,b] Jae-Won Huh,[f] Yong Chul Bae,[g] Dong-Seok Lee[a,b]

[a]School of Life Science, BK21 Plus KNU Creative BioResearch Group, Kyungpook National University, Daegu, Republic of Korea
[b]College of Natural Sciences, Kyungpook National University, Daegu, Republic of Korea
[c]College of Medicine, Chungbuk National University, Chungbuk, Republic of Korea
[d]Department of Radiology, Chungbuk National University Hospital, Chungbuk, Republic of Korea
[e]Research Institute, e-biogen Inc., Seoul, South Korea
[f]National Primate Research Center, Korea Research Institute of Bioscience and Biotechnology (KRIBB), Cheongju, Republic of Korea
[g]Department of Anatomy and Neurobiology, School of Dentistry, Kyungpook National University, Daegu, Republic of Korea

ABSTRACT Glutamate is an essential neurotransmitter in the central nervous system (CNS). However, high glutamate concentrations can lead to neurodegenerative diseases. A hallmark of glutamate toxicity is high levels of reactive oxygen species (ROS), which can trigger Ca^{2+} influx and dynamin-related protein 1 (Drp1)-mediated mitochondrial fission. Peroxiredoxin 5 (Prx5) is a well-known cysteine-dependent peroxidase enzyme. However, the precise effects of Prx5 on glutamate toxicity are still unclear. In this study, we investigated the role of Prx5 in glutamate-induced neuronal cell death. We found that glutamate treatment induces endogenous Prx5 expression and Ca^{2+}/calcineurin-dependent dephosphorylation of Drp1, resulting in mitochondrial fission and neuronal cell death. Our results indicate that Prx5 inhibits glutamate-induced mitochondrial fission through the regulation of Ca^{2+}/calcineurin-dependent dephosphorylation of Drp1, and it does so by scavenging cytosolic and mitochondrial ROS. Therefore, we suggest that Ca^{2+}/calcineurin-dependent mitochondrial dynamics are deeply associated with glutamate-induced neurotoxicity. Consequently, Prx5 may be used as a potential agent for developing therapies against glutamate-induced neurotoxicity and neurodegenerative diseases where it plays a key role.

KEYWORDS Ca^{2+}, calcineurin, HT22, mitochondria, peroxiredoxin 5, ROS, glutamate

Glutamate, an important endogenous neurotransmitter in the mammalian central nervous system (CNS), acts as a crossroad in neuronal cell signaling in processes such as differentiation, migration, and survival (1). However, high concentrations of extracellular glutamate lead to neuronal cell death by excitotoxicity. Glutamate-mediated neuronal cell death contributes to critical neurodegenerative disorders, including brain trauma, cerebral ischemia, epilepsy, stroke, Parkinson's disease, and Alzheimer's disease (2–4). Several studies have reported that glutamate-mediated excitotoxicity is closely associated with the activation of glutamate receptors and nonglutamate receptor toxicity. There are three types of glutamate ionotropic receptors, *viz.*, α-amino-3-hydroxy-5-methyl-4-isoxazolepropionic acid (AMPA), kainate, and *N*-methyl-D-aspartate (NMDA). These receptors are widely distributed in the cortex, the ventral striatum, and the hippocampus, respectively, at various concentrations (5). Nonglutamate receptor toxicity occurs via the overproduction of reactive oxygen species (ROS), the excessive influx of calcium (Ca^{2+}), and the following neurotoxic cascades without the involve-

Citation Kim MH, Lee HJ, Lee S-R, Lee H-S, Huh J-W, Bae YC, Lee D-S. 2019. Peroxiredoxin 5 inhibits glutamate-induced neuronal cell death through the regulation of calcineurin-dependent mitochondrial dynamics in HT22 cells. Mol Cell Biol 39:e00148-19. https://doi.org/10.1128/MCB.00148-19.

Copyright © 2019 American Society for Microbiology. All Rights Reserved.

Address correspondence to Dong-Seok Lee, lee1@knu.ac.kr.

Received 2 April 2019
Returned for modification 21 May 2019
Accepted 21 July 2019
Accepted manuscript posted online 29 July 2019
Published 27 September 2019

ment of the glutamate receptor (6–8). Excessive ROS derived from the mitochondria induces oxidative stress, and it plays an active role in the early and late steps of apoptosis regulation. Notably, ROS causes a rapid Ca^{2+} influx, intracellular Ca^{2+} overload, and mitochondrial membrane depolarization, which leads to additional ROS generation and secondary messenger/enzyme activation, which eventually trigger neuronal cell death (9, 10). The release and translocation of the apoptosis-inducing factor from the mitochondria to the cytosol initiate the subsequent events related to apoptosis, including up/downregulation of Bax and Bcl-2, release of cytochrome *c*, activation of caspase-3, and cleavage of poly(ADP-ribose) polymerase 1 (PARP-1) (11, 12). Previous studies have emphasized that controlling ROS production and Ca^{2+} influx may be an effective therapeutic strategy for neurodegenerative diseases (13, 14).

Peroxiredoxins (Prxs), a family of cysteine-dependent peroxidase enzymes, play a crucial role in scavenging peroxide and peroxynitrite in mammalian cells. Prxs are categorized as Prx1 to Prx6 depending on their subcellular localization. Notably, since Prx5 is located within the cytosol and the mitochondria, it can effectively remove intracellular ROS (15). Previous studies have determined that Prx5 is a potent antioxidant enzyme that contributes to cellular homeostasis by scavenging intracellular ROS (16–19). However, the role of Prx5 in protection against glutamate-induced neuronal cell death remains unclear. The distribution of Prxs in mammalian tissues has been reported. In the brain tissue, Prx2 is expressed in the habenular nuclei of the hypothalamus, whereas Prx1 and Prx6 are expressed in the astrocyte and microglia. Prx5 in particular is observed in the hippocampus (20). These findings imply that Prx5 is essential for the functional maintenance of the hippocampus and is related to neurodegenerative diseases.

Mitochondria are very dynamic cytoplasmic organelles that experience successive fission/fusion events (mitochondrial dynamics) and are involved in the production of ATP and the regulation of intracellular Ca^{2+} (21, 22). Mitochondrial dynamics are primarily controlled by mitochondrial fission and fusion proteins. Some of these proteins are dynamin-related protein 1 (Drp1), mitochondrial fission 1 protein (Fis1), mitofusin-1 and -2 (Mfn1 and Mfn2), and Opa1. Drp1 and Fis1 regulate mitochondrial fission, and Mfn1, Mfn2, and Opa1 regulate mitochondrial fusion (23). Several studies have reported that the imbalance of mitochondrial fission/fusion accelerates mitochondrial fragmentation and dysfunction and is closely associated with neuronal cell death (24–26). Drp1 activity, which is controlled by its phosphorylation/dephosphorylation, functions as a key regulator of mitochondrial functions, and modulating Drp1 activity can inhibit glutamate-induced neuronal cell death (27, 28). In particular, the dephosphorylation of the 637th serine residue in Drp1 induces the translocation of Drp1 to mitochondria, where it promotes mitochondrial fission and, in turn, apoptosis (29). This residue is dephosphorylated by calcineurin, which is a Ca^{2+}/calmodulin-dependent serine/threonine phosphatase and comprises the family of protein phosphatase 2B (30). A previous study has reported that Ca^{2+}/calmodulin-dependent protein kinase I (CaMK I), a CaMK II family member, phosphorylates the 637th serine residue of Drp1 in the brain (31). Therefore, the precise mechanisms that control the activation of calcineurin may be important for neurodegenerative diseases. In this study, we investigated the role of Prx5 and ROS in glutamate-induced neuronal death using mouse hippocampal HT22 cells. In addition, we also demonstrated mitochondrial dynamics and the calcineurin pathway in glutamate-induced neuronal cell death. In this study, we determined that Prx5 protected HT22 cells from glutamate-induced cell death by scavenging ROS. We further demonstrated that Prx5 attenuated mitochondrial fission by inhibiting the calcineurin pathway. Our results suggest that Prx5 exerts a protective effect on glutamate-induced neuronal cell death, implying that Prx5 is a potential agent for the treatment of neurodegenerative diseases.

RESULTS

Glutamate induces expression of apoptosis-related proteins in HT22 cells. Glutamate-induced excitotoxicity is well known to induce neuronal cell death (32). First,

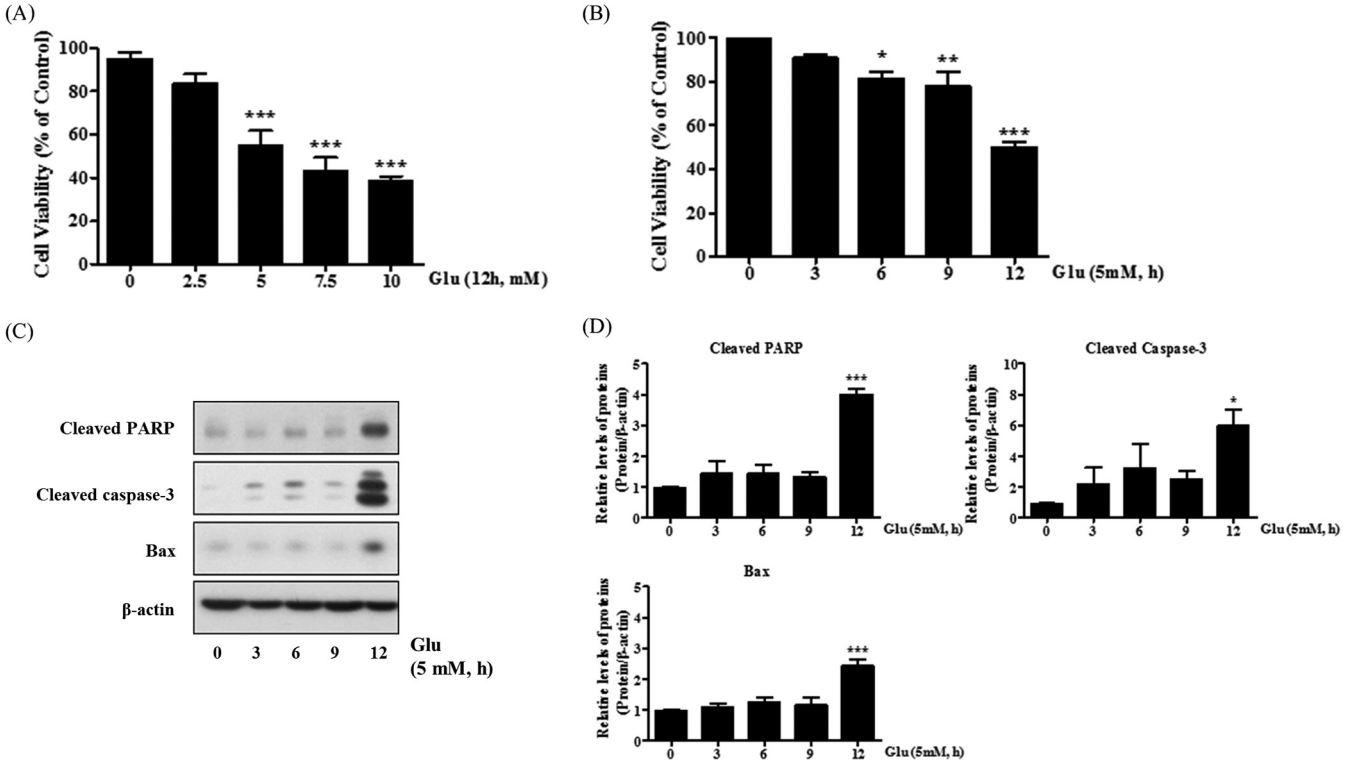

FIG 1 Increased cell death and ROS generation after glutamate treatment in HT22 cells. HT22 cells were treated with 5 mM glutamate for up to 12 h. (A and B) Cell viability was measured with the MTT reduction assay in a glutamate dose- or time-dependent manner. (C and D) Expression of apoptotic proteins (cleaved PARP, cleaved caspase-3, and Bax) was detected by Western blotting. Untreated HT22 cells were used as a negative control. Values are presented as means ± SD ($n = 3$). *, $P < 0.05$; **, $P < 0.01$; ***, $P < 0.001$; each versus the control.

using the 3-(4,5-dimethyl-2-thiazolyl)-2,5-diphenyl-2H-tetrazolium bromide (MTT) assay, we confirmed that glutamate treatment decreased cell viability in a concentration-dependent manner; the 50% inhibitory concentration (IC_{50}) values were 5 mM (Fig. 1A). We also performed a time-based MTT assay and observed that the viability of HT22 cells decreased to approximately 50% after 12 h of treatment with 5 mM glutamate (Fig. 1B). We next examined the change in the expression of apoptosis-related proteins, including cleaved PARP, cleaved caspase-3, and Bax, using Western blot analysis. As shown in Fig. 1C and D, the expression of apoptosis-related proteins was significantly upregulated in HT22 cells treated with glutamate.

Prx5 expression is induced by glutamate treatment in an ROS-dependent manner. Using 2,7-dichlorofluorescein diacetate (CM-H_2DCF-DA) and MitoSOX staining, we investigated whether glutamate induced intracellular or mitochondrial reactive oxygen species (ROS) accumulation, respectively (Fig. 2A and B). We observed that glutamate increased the levels of intracellular and mitochondrial ROS, indicating that glutamate-induced neuronal cell death is associated with an increase in ROS generation. We next treated HT22 cells with glutamate for 3, 6, 9, and 12 h to determine whether the increase of ROS levels induced by glutamate has an effect on the expression of peroxiredoxins (Fig. 2C and D). With increased glutamate treatment time, we observed a slight increase in the levels of Prx1 to Prx6 (Prx1-6). Notably, Prx5 was significantly upregulated after 12 h of glutamate treatment. Altogether, these results indicate that the glutamate-dependent increase of Prx5 is closely linked to glutamate-induced ROS generation and that Prx5 has the potential to protect HT22 cells from glutamate-induced apoptosis.

Prx5 protects HT22 cells against glutamate-induced cell death through the regulation of ROS generation. To evaluate the effects of Prx5 on glutamate-induced apoptosis, we created HT22 cell lines stably expressing Prx5 (V5 tagged) or siPrx5

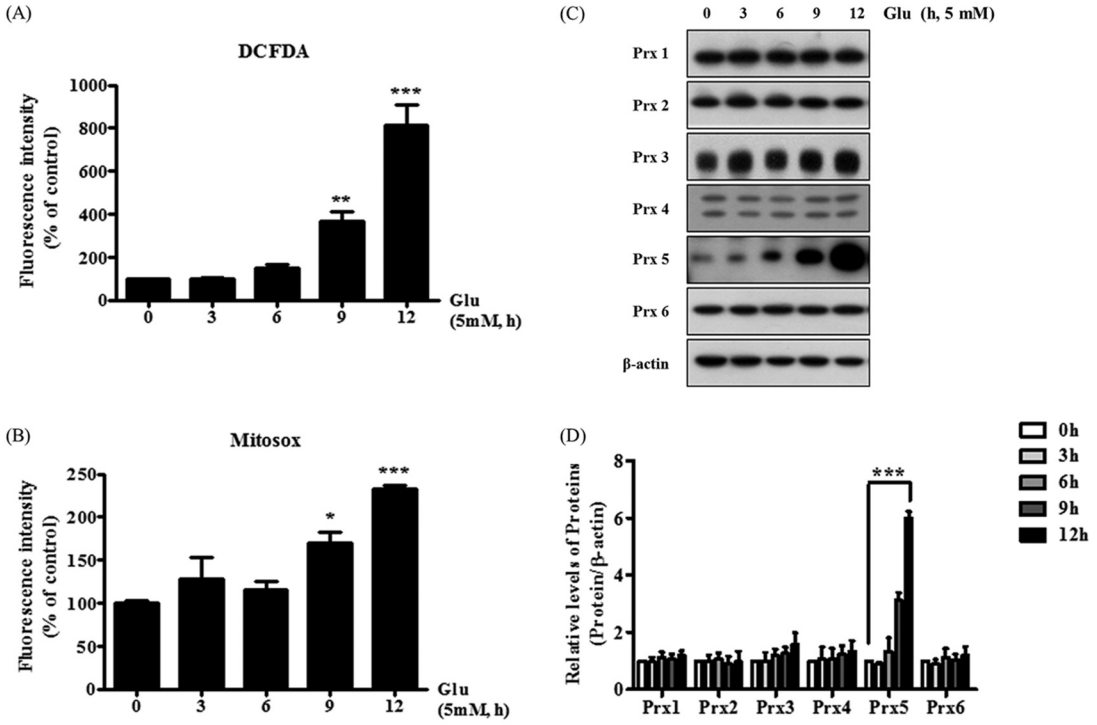

FIG 2 Effects of glutamate on the production of reactive oxygen species (ROS) and the expression of peroxiredoxins (Prxs). HT22 cells were incubated with 5 mM glutamate for up to 12 h. (A) Intracellular ROS levels were detected with the 2,7-dichlorofluorescein diacetate (CM-H2DCF-DA) assay. (B) Mitochondrial ROS levels were detected with MitoSOX staining. (C and D) Western blotting was used to measure the expression level of peroxiredoxins (Prxs). Untreated HT22 cells were used as a negative control. Values are presented as means ± SD ($n = 3$). *, $P < 0.05$; **, $P < 0.01$; ***, $P < 0.001$; each versus the control.

(silenced Prx5). To begin, we confirmed the expression of Prx5 by Western blotting with Prx5 and V5 tag antibodies. Indeed, our results showed that exogenous and endogenous Prx5 was successfully overexpressed in HT22-Prx5 cells and silenced in HT22-siPrx5 cells, respectively (Fig. 3A). We next examined ROS levels, which are closely related to cell death, using oxidative-reactive fluorescent dyes. We used H_2DCF-DA, which is specific to intracellular ROS, and MitoSOX, which is specific to mitochondrial ROS. As shown in Fig. 3B and C, we observed that Prx5 overexpression mildly attenuated intracellular and mitochondrial glutamate-induced ROS generation, whereas Prx5 silencing increased glutamate-induced ROS generation. These results indicate that the ROS scavenging activity of Prx5 protects HT22 cells from glutamate toxicity. In addition, we determined the cell viability of HT22, HT22-Prx5, and HT22-siPrx5 cells treated with glutamate using the MTT assay. We observed that the cell viability (relative to that of untreated HT22 cells) was higher in HT22-Prx5 cells treated with glutamate than in HT22-siPrx5 and HT22 cells treated with glutamate (Fig. 3D). Subsequently, a quantitative evaluation of apoptosis was carried out via flow cytometry with annexin V/propidium iodide (PI) staining. Notably, the rate of apoptosis after glutamate treatment was lower in cells stably expressing Prx5 than in HT22-siPrx5 and HT22 cells (Fig. 3E). Accordingly, Prx5 overexpression inhibited the cleavage of caspase-3 (Fig. 3F). In contrast to HT22-Prx5 cells, HT22-siPrx5 cells displayed markedly lower cell viability, increased apoptotic cell rate, and high levels of cleaved caspase-3. Overall, our results imply that Prx5 prevents glutamate-induced cell death, which is linked to apoptosis, by regulating excessive ROS generation.

Prx5 prevents glutamate-induced mitochondrial fission by regulating Drp1 phosphorylation. Glutamate-induced apoptosis is usually accompanied by mitochondrial fission (33). To investigate whether Prx5 is involved in the change of mitochondrial morphology, we established HT22 and HT22-siPrx5 cell lines stably expressing DsRed2-mito and an HT22 cell line stably coexpressing DsRed2-mito and Prx5. Via confocal

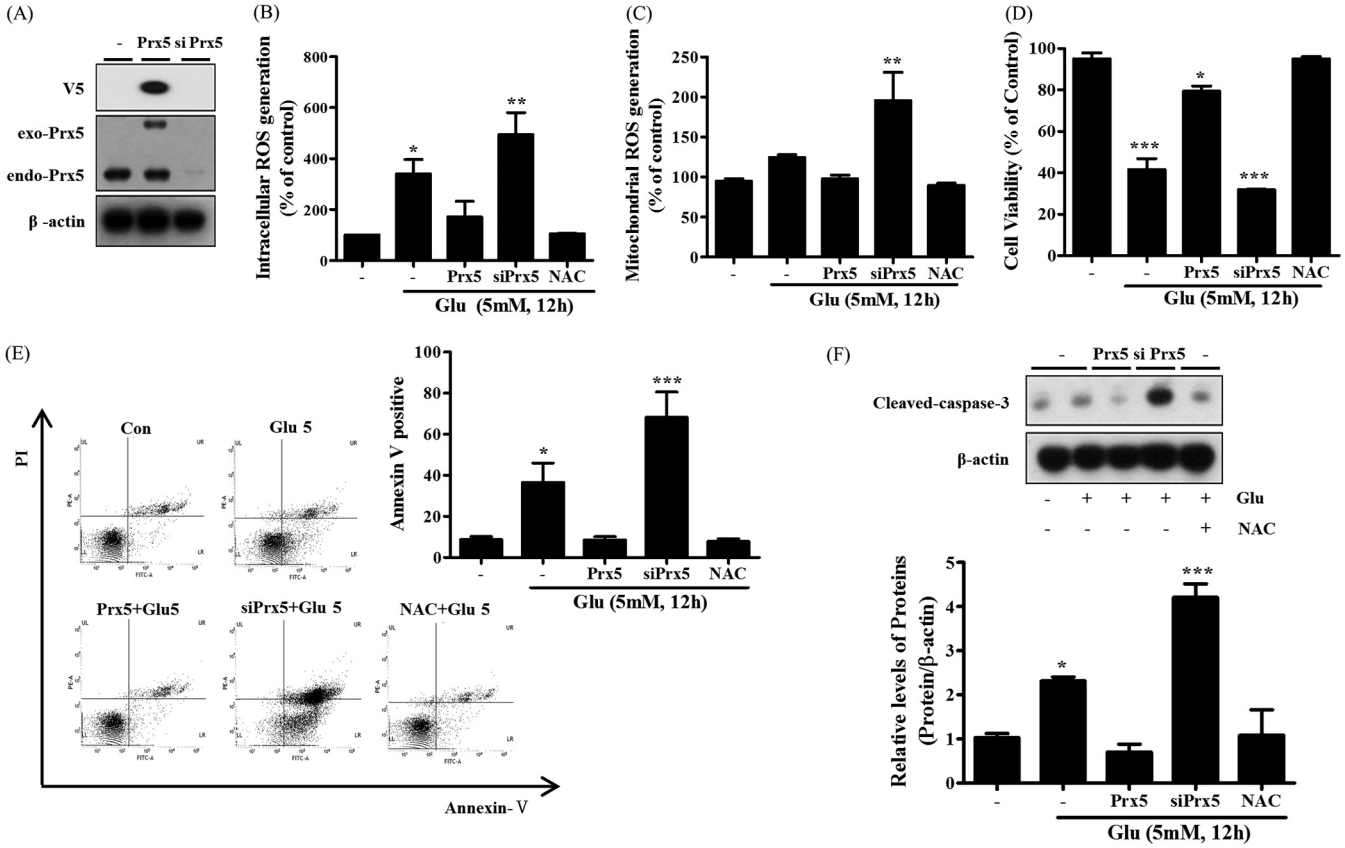

FIG 3 Protective effect of Prx5 in glutamate-induced apoptosis. After treating HT22 cells with 5 mM glutamate for 12 h, we detected intracellular ROS levels. HT22 cells treated with 10 mM *N*-acetyl-L-cysteine (NAC) were used as a positive control. (A) Stable expression of exogenous Prx5 and silenced Prx5 (siPrx5) was detected in HT22 cells by Western blotting with Prx5 and V5 tag antibodies. (B and C) Flow cytometry analysis of intracellular ROS levels (detected with CMH_2DCF-DA) and mitochondrial ROS levels (detected with MitoSOX) in HT22, HT22-Prx5, and HT22-siPrx5 cells treated with glutamate. (D) Cell viability was assessed with the MTT assay in HT22, HT22-Prx5, and HT22-siPrx5 cells treated with glutamate. (E) Flow cytometry analysis of cell apoptosis using annexin V-FITC/PI dual staining and the derived histogram showing the percentage of apoptotic cells calculated by densitometry. (F) Expression level of cleaved caspase-3 was measured by Western blotting (exo-Prx5, exogenous Prx5; endo-Prx5; endogenous Prx5). Untreated HT22 cells were used as a control. Values are presented as means ± SD ($n = 3$). *, $P < 0.05$; **, $P < 0.01$; ***, $P < 0.001$; each versus the control.

microscopy, we then observed the morphology of the mitochondria in these three types of HT22 cells after glutamate treatment for 12 h. Our results showed that Prx5-overexpressing HT22 cells had a more elongated mitochondrial morphology than HT22 and HT22-siPrx5 cells. In particular, HT22-siPrx5 cells showed severely damaged and fragmented mitochondrial morphology (Fig. 4A). Also, we assessed the levels of phosphorylation of Drp1 (Ser637), which is implicated in mitochondrial fission. As shown in Fig. 4B, the p-Drp1 (Ser637) levels decreased after glutamate treatment was restored to control (untreated) levels by Prx5 overexpression, whereas Prx5 silencing downregulated p-Drp1 (Ser637) levels after glutamate treatment. However, we did not detect any significant change in the expression of other proteins related to mitochondrial fusion (Mfn1 and Mfn2). Altogether, these results suggest that Prx5 inhibits glutamate-induced mitochondrial fission by modulating the phosphorylation of Drp1 (Ser637).

Prx5 inhibits the dephosphorylation of Drp1 by regulating Ca^{2+}-mediated calcineurin activation. The dephosphorylation of Drp1 at serine 637 is mediated by Ca^{2+}-dependent calcineurin activation. Intracellular Ca^{2+} accumulation induces the cleavage and activation of calcineurin by promoting the interaction of calmodulin with subunit A of calcineurin (CnA) (34). Therefore, we investigated the impact of Prx5 expression on calcineurin activation by quantifying the cleavage of calcineurin. Before assessing calcineurin activation, we measured intracellular Ca^{2+} levels by flow cytometry using Fluo-4 AM after glutamate treatment. Our results showed that intracellular

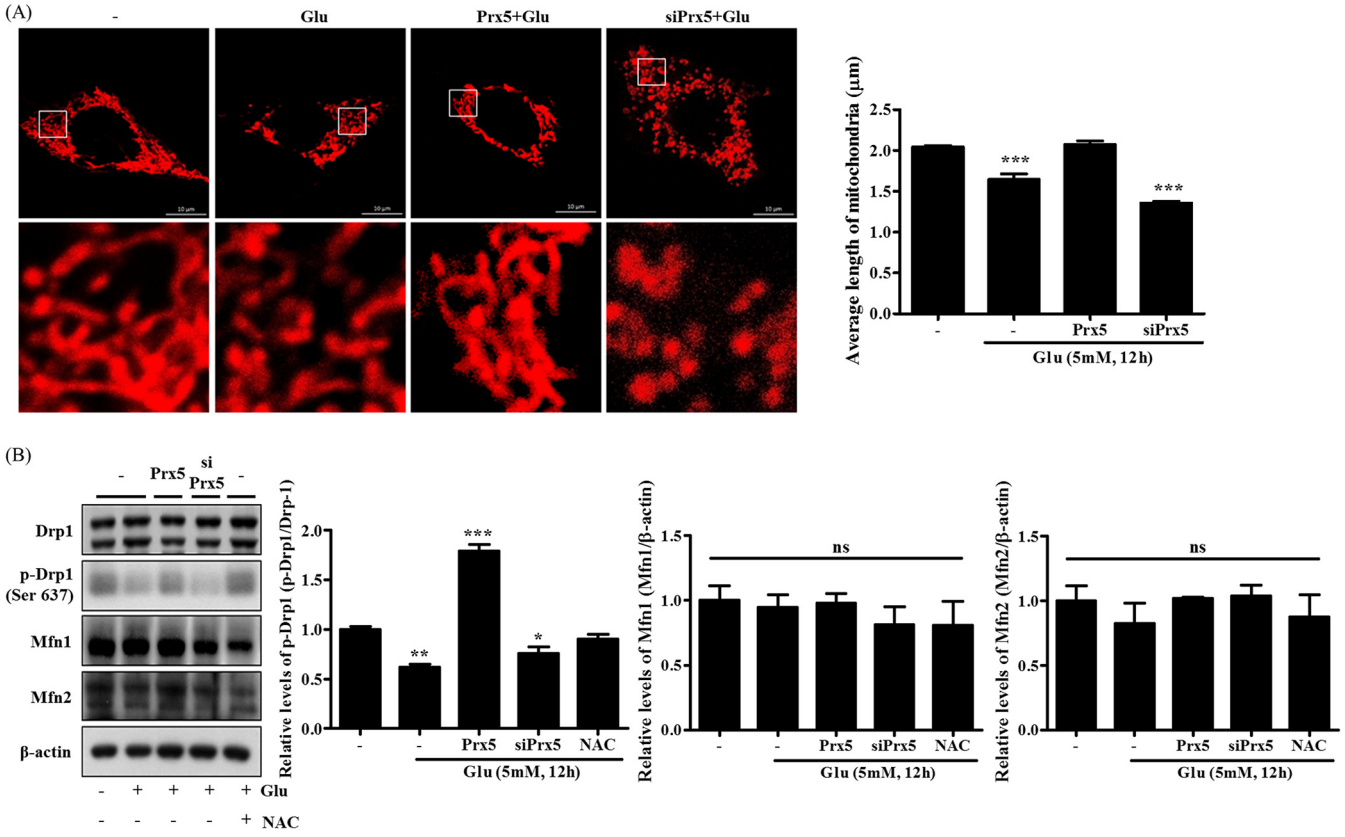

FIG 4 Positive regulation of glutamate-induced mitochondrial dysfunction by Prx5. The three types of cells (HT22, HT22-Prx5, and HT22-siPrx5) were treated with 5 mM glutamate for 12 h. HT22 cells treated with 10 mM *N*-acetyl-L-cysteine (NAC) were used as the positive control. (A) Confocal microscopy images depicting the change in mitochondrial morphology induced by glutamate treatment in HT22 and HT22-siPrx5 cells stably expressing DsRed2-mito and HT22 cells stably coexpressing DsRed2-mito and Prx5. The images in the second row correspond to a higher magnification of the area within the white square in the images in the first row. The histogram below the images shows the quantification of the average mitochondrial length. Mitochondrial lengths were analyzed based on individual mitochondria. (B) The molecular footprint of mitochondrial dynamics was determined by Western blotting with Drp1, p-Drp1 (Ser 637), Mfn1, and Mfn2 antibodies. Untreated HT22 cells were used as a control. Values are presented as means ± SD ($n = 3$). *, $P < 0.05$; **, $P < 0.01$; ***, $P < 0.001$; ns, not significant; each versus the control.

Ca^{2+} levels increased along with an increase in glutamate treatment time (Fig. 5A). We then confirmed the effect of Prx5 expression on glutamate-induced Ca^{2+} accumulation; as shown in Fig. 5B, Prx5 remarkably reduced intracellular Ca^{2+} levels, whereas siPrx5 significantly increased Ca^{2+} levels. We next assessed the levels of cleaved calcineurin in the presence of glutamate with or without the calcineurin inhibitor cyclosporine (CsA) and the Ca^{2+} chelator 1,2-bis(*o*-aminophenoxy)ethane-*N*,*N*,*N*′,*N*′-tetraacetic acid (BAPTA) (Fig. 5C). We found that Prx5 overexpression effectively blocked the increase in calcineurin cleavage, whereas siPrx5 increased the levels of cleaved calcineurin. As expected, inhibition of calcineurin and chelation of Ca^{2+} slightly decreased the expression of cleaved calcineurin. These results indicate that Prx5 inhibits the activation of calcineurin by regulating intracellular Ca^{2+} accumulation.

Subsequently, we analyzed the change in mitochondrial morphology induced by CsA and BAPTA in HT22 and HT22-siPrx5 cells expressing DsRed2-mito. We observed that the inhibition of calcineurin activity and Ca^{2+} accumulation rescued glutamate-induced mitochondrial fission regardless of whether endogenous Prx5 was expressed (Fig. 5D). This result suggests that the severe mitochondrial fission induced by silencing Prx5 depends on the Ca^{2+} influx and calcineurin activation. In addition, we found that CsA and BAPTA reversed the glutamate-induced dephosphorylation of Drp1 (Ser 637) and the cleavage of caspase-3 (Fig. 5E and F). Therefore, it is likely that Prx5 prevents glutamate-induced apoptosis by controlling the levels of intracellular Ca^{2+} and calcineurin activity upstream of Drp1.

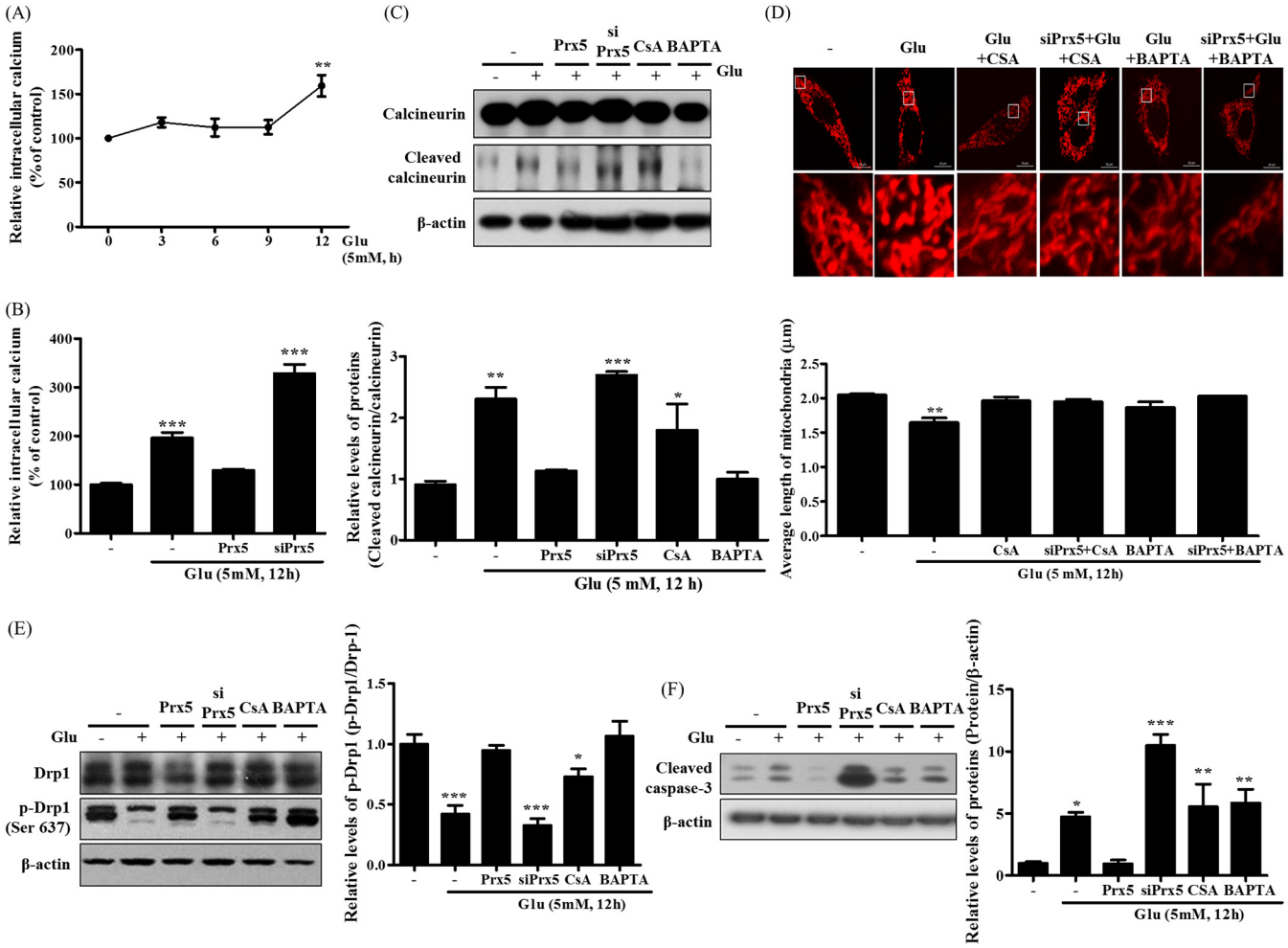

FIG 5 Effect of Prx5 on glutamate-induced calcineurin activation through regulating Ca^{2+} level in HT22 cells. Three types of cells were treated with 5 mM glutamate for 12 h in the presence or absence of CsA (1 μM) or BAPTA (0.25 μM). (A) The change of intracellular Ca^{2+} level in a time-dependent manner was detected with Fluo-4 AM. (B) The levels of intracellular Ca^{2+} in HT22, HT22-Prx5, and HT22-siPrx5 cells were detected with Fluo-4 AM. (C) The levels of calcineurin and cleaved calcineurin were assessed by Western blotting. (D) The changes in mitochondrial morphology after glutamate treatment were observed by confocal microscopy. The images in the second row correspond to a higher magnification of the area within the white square in the images in the first row. The histogram below the images shows the quantification of the average mitochondrial length. Mitochondrial lengths were analyzed based on individual mitochondria. (E) The alteration of mitochondrial dynamics was characterized by assessing the levels of Drp1 and p-Drp1 (Ser 637) by Western blotting. (F) Expression level of cleaved caspase-3 was assessed by Western blotting. Untreated HT22 cells were used as a control. Values are presented as means ± SD ($n = 3$). *, $P < 0.05$; **, $P < 0.01$; ***, $P < 0.001$; each versus the control.

DISCUSSION

To determine whether Prx5 has a protective effect against glutamate neurotoxicity, we established two HT22 cell lines: one that stably overexpressed Prx5 and one that silenced endogenous Prx5 expression (Fig. 3A). This study's results demonstrate that Prx5 overexpression effectively protected HT22 cells from glutamate-induced neurotoxicity through the regulation of intracellular ROS levels and excessive calcium influx (Fig. 3 and 5). In addition, we showed that Prx5 rescued seriously damaged mitochondrial morphology by controlling the expression of mitochondrial fusion/fission proteins. Notably, overexpression of Prx5 blocked the dephosphorylation of Drp1 (Ser 637) by modulating Ca^{2+}-calcineurin signaling (Fig. 5). On the other hand, knockdown of Prx5 aggravated glutamate-induced neurotoxicity (Fig. 4). These findings suggest that Prx5 has a protective effect against glutamate-induced cell death in hippocampal neuronal HT22 cells (Fig. 6).

The Prx family is a large family of cysteine-dependent peroxidases that reduce hydrogen peroxide (H_2O_2), peroxynitrite, and alkyl hydroperoxides, thereby contribut-

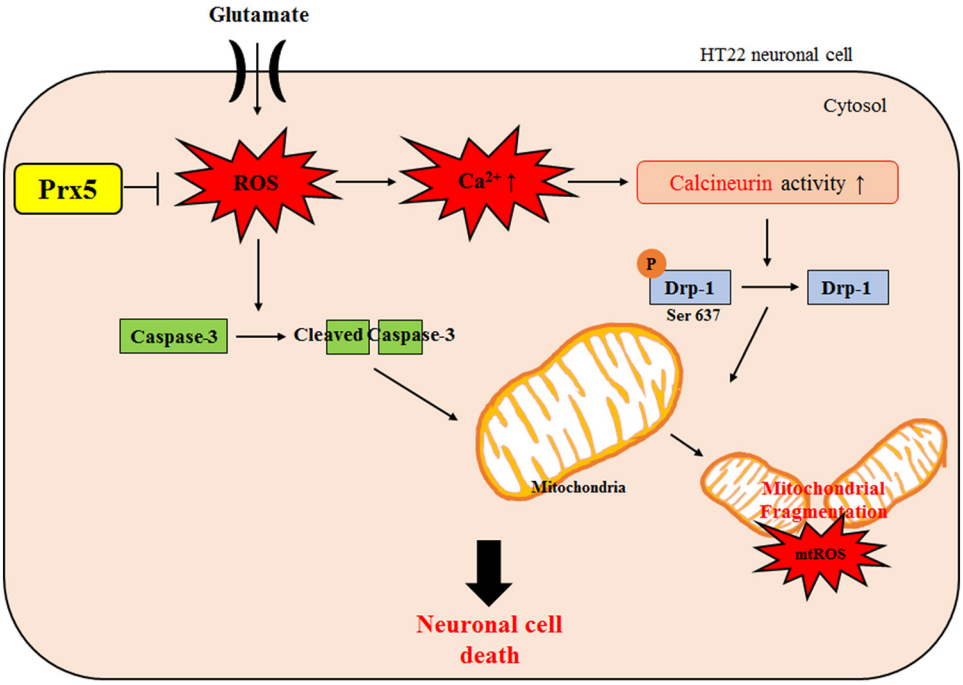

FIG 6 Proposed schematic of the Prx5 protective effect against glutamate-induced toxicity in HT22 cells.

ing to redox balance in mammalian cells. The Prx family has 6 subtypes (Prx1-6), each with a characteristic subcellular localization. Prx1, Prx2, and Prx6 are strongly expressed in the cytosol, Prx3 in the mitochondria, Prx4 in the endoplasmic reticulum, and Prx5 in both the cytosol and mitochondria (35, 36). There are numerous studies about the relationship between the Prx family and oxidative stress (37–40). In particular, Prx5 has been shown to have intensive antioxidant effects in various cellular systems, such as cancer cells, immune cells, neuronal cells, and adipocytes (17–19, 41, 42). Notably, Prx5 is an essential antioxidant for maintaining the redox balance in neuronal cells (43). However, the precise relationship between Prx5 and glutamate-induced ROS is still unknown. Therefore, we focused on the role of Prx5 in HT22 cells, the immortalized mouse hippocampal neuronal cell model. In the present study, although the expression of all Prxs was slightly increased by glutamate treatment in HT22 cells, Prx5 was expressed more than other Prxs, suggesting the important role of Prx5 in glutamate-induced neurotoxicity (Fig. 2). We demonstrated that Prx5 overexpression inhibited glutamate-induced cell death by preventing intracellular and mitochondrial ROS production (Fig. 3). These findings suggest that Prx5 can stabilize redox balance in glutamate-induced neuronal cell death.

Glutamate is a well-known neurotransmitter in the CNS. However, excessive glutamate accumulation can not only damage neuronal signaling functions but also trigger cell death through excitotoxicity (44). Excitotoxicity is a major cause of several neurodegenerative diseases, such as Alzheimer's disease, Huntington's disease, lateral amyotrophic sclerosis, Parkinson's disease, hypoglycemia, epilepsy, stroke, and traumatic brain injury (45–47). Glutamate-mediated excitotoxicity is triggered by the activation of the NMDA receptor or the AMPA receptor or by the activation of nonglutamate receptors mediated by oxidative stress (14, 48). Glutamate toxicity results in different reactions based on the cell types and the existence of glutamate receptors (49). In the present study, we used HT22 cells, which lack functional glutamate receptors, to study glutamate-induced oxidative neurotoxicity. The HT22 cell line is widely used to study non-receptor-mediated glutamate toxicity. We showed that glutamate treatment decreased cell viability and induced cleavage of caspase-3 in HT22 cells (Fig. 1); this finding confirms that the observed glutamate-induced cell death was due to apoptosis.

Oxidative neurotoxicity is accompanied by high levels of glutamate, resulting in inhibition of cysteine uptake and depletion of intracellular glutathione (GSH). In neuronal cells, it can lead to increased ROS and nitric oxide (NO) production, expression of cytotoxic transcription factors, and damaged intracellular Ca^{2+} homeostasis (excessive Ca^{2+} influx) (50). Previous studies have addressed the neuroprotective effects of antioxidant enzymes using cell models overexpressing ROS-related enzymes like Cu/Zn superoxide dismutase 1 (SOD1), SOD2, and Prx6 (51–53). In addition, there are several studies that show that immoderate ROS production is closely related to unstable Ca^{2+} homeostasis (54). Results from our study also showed that glutamate treatment increased intracellular and mitochondrial ROS and Ca^{2+} accumulation in HT22 cells (Fig. 2 and 5A). Also, we showed that Prx5 overexpression remarkably decreased ROS level and intracellular Ca^{2+} levels in glutamate-treated HT22 cells, whereas Prx5 silencing resulted in the opposite (Fig. 3B and C and 5B). These results support the hypothesis that Prx5 can prevent neuronal cell death by blocking ROS generation and Ca^{2+} influx and imply that glutamate-induced neurotoxicity is associated with ROS generation and Ca^{2+} influx. Moreover, Ca^{2+} influx stimulates mitochondrially localized Nox2 (homolog of NADPH oxidase), which contributes to ROS generation in cells.

Mitochondria are dynamic organelles that undergo continuous mitochondrial fission/fusion (called mitochondrial dynamics) to maintain their functions in cellular energy metabolism, Ca^{2+} signaling, and generation of ROS (55, 56). Therefore, the equilibrium of mitochondrial fission and fusion is crucial for cellular homeostasis. Several factors are tightly linked and involved in mitochondrial dynamics. Mitochondrial fusion is regulated by Mfn1, Mnf2, and Opa1. Mfn1 and Mfn2 participate in the fusion of outer mitochondrial membranes, whereas Opa1 participates in the fusion of inner mitochondrial membranes. Mitochondrial fission is regulated by Drp1 through interaction with the mitochondrial receptor protein Fis1. Fis1 mediates the binding of Drp1 to the mitochondrial membrane (57, 58). Drp1-mediated mitochondrial dynamics depend on the phosphorylation status of Drp1. The activity of Drp1 is determined by protein kinase A (PKA) and calcineurin activation (30, 59). Calcineurin-dependent dephosphorylation of the 637th serine residue in Drp1 inhibits mitochondrial fusion, eventually causing mitochondrial fragmentation and dysfunction (30). In the current study, we examined the calcineurin-dependent dephosphorylation of Drp1 (Ser 637) and change of mitochondrial morphology in glutamate-treated HT22, HT22-Prx5, and HT22-siPrx5 cells. As expected, our results showed that Prx5 overexpression inhibited dephosphorylation of Drp1 and the cleavage of calcineurin. Furthermore, we observed that Prx5 prevented glutamate-induced mitochondrial fission, whereas knockdown of Prx5 (siPrx5) enhanced mitochondrial fission through calcineurin-dependent dephosphorylation of Drp1 (Fig. 4 and 5). Moreover, when we cotreated with glutamate and CsA (calcineurin inhibitor)/BAPTA (Ca^{2+} chelator), we observed that mitochondrial morphology recovered despite glutamate treatment. These results support the hypothesis that glutamate-induced mitochondrial fragmentation is triggered by the Ca^{2+}/calcineurin pathway. Consistent with this hypothesis, after treatment with glutamate, HT22-siPrx5 cells displayed severely fragmented mitochondrial morphology and increased apoptotic rates compared with those of control HT22 cells. On the contrary, Prx5 overexpression protected HT22 cells from glutamate-induced cell death (Fig. 3 and 4). Overall, these results demonstrate that mitochondrial fission induced by glutamate treatment aggravates apoptosis and that Prx5 regulates mitochondrial dynamics by modulating calcineurin activity.

In conclusion, our study provides valuable information regarding the relationship between Prx5 and glutamate-induced neuronal death and explains the need to further study Prx5 for its potential applications in neurodegenerative diseases. Taken together, our data indicate that Prx5 can alleviate severe mitochondrial fission and improve glutamate-induced apoptosis through inhibiting ROS-dependent Ca^{2+}/calcineurin signaling and dephosphorylation of Drp1 (Ser 637) in HT22 cells (lacking specific glutamate receptors). Furthermore, based on these results, we hypothesize that Prx5 exerts a protective effect against excitotoxicity in other neuronal cell lines that have glutamate

receptors. In future studies, we will focus on the relationship between Prx5 and glutamate receptor-mediated excitotoxicity. In summary, these findings suggest that Prx5 acts as a crucial regulator in glutamate-induced neurotoxicity and that it may be used in the treatment of neurodegenerative diseases.

MATERIALS AND METHODS

Chemicals and reagents. Glutamate, CsA, and BAPTA were purchased from Sigma-Aldrich (MO). Dulbecco's modified Eagle's medium (DMEM) and penicillin-streptomycin were purchased from Welgene (Daegu, South Korea).

Cell culture and glutamate treatment. Mouse hippocampal neuronal HT22 cells were cultured at 5% CO_2 and 37°C in DMEM containing 4,500 mg/liter glucose and supplemented with 1% penicillin-streptomycin and 10% fetal bovine serum (FBS; Gibco, New Zealand). For the glutamate treatment, the cells were cultured in 6-well plates (SPL Life Sciences Co., Pocheon-si, South Korea), and 12 h later, the cells were incubated with 5 mM glutamate (Sigma-Aldrich, MO) for 12 h.

Plasmid cloning and establishment of stable Prx5-expressing HT22 cell line. The Prx5 gene was provided by Tae-Hoon Lee (Chonnam National University, Gwangju, South Korea). The Prx5 coding sequence was amplified by PCR using LA *Taq* polymerase (TaKaRa, Shiga, Japan) and cloned into the pCR8/GW/TOPO vector (Invitrogen, CA). The Prx5 gene then was inserted into pLenti6.3/V5-DEST using LR clonase (Invitrogen). This particular vector encodes a 14-amino-acid V5 epitope at the C terminus that helps in the detection of recombinant proteins during immunoblot analysis (60). Therefore, although mammalian Prx5 is about 17 kDa in molecular size (61), it ends up being detected as more than 20 kDa in size. To establish a stable cell line, HT22 cells were seeded in 6-well plates. After 24 h, the cells were transfected with 2 μg of pLenti6.3-DsRed2-Mito and pLenti6.3-Prx5 using Effectene (Qiagen, CA) according to the manufacturer's instructions. After 24 h, the transfected cells were selected using 8 μg/ml blasticidin (Invitrogen) for 7 days.

RNA interference assay. Once the HT22 cells reached 50% confluence, they were transfected with 10pmol of short interfering RNA (siRNA) against Prx5 (siPrx5; Bioneer, Daejeon, South Korea) using Lipofectamine RNAiMAX (Thermo Fisher Scientific, MA) as previously described (16, 62). The siRNA sequences were the following: siPrx5 sense, 5′-GUCUGAGCGUUAAUGACGU-3′; siPrx5 antisense, 5′-ACG UCAUUAACGCUCAGAC-3′.

Analysis of cell viability. Cell viability was measured with the MTT assay; HT22 cells (density, 5×10^3 cells for each cell type) were cultured in 6-well plates for 12 h before treatment with glutamate. The cells were then incubated with 5 mM glutamate for 12 h. The culture medium then was carefully removed and replaced with 0.5 mg/ml MTT solution dissolved in phenol red-free DMEM. The cells were then incubated for 1 h at 37°C. The medium next was removed, and 500 μl dimethyl sulfoxide (DMSO) was added to each well to dissolve the formazan crystals. Absorbance was measured at 550 nm with an Infinite F50 microplate reader (TECAN, Männedorf, Switzerland).

Flow cytometry. Intracellular and mitochondrial ROS were detected using 2,7-dichlorofluorescein diacetate (CM-H_2DCF-DA; Invitrogen) and MitoSOX Red (Molecular Probes, OR), respectively. Intracellular calcium levels were measured by using Fluo-4 AM (Thermo Fisher Scientific). HT22, HT22-Prx5, and HT22-siPrx5 cells were seeded in 6-well plates. Following 12 h of incubation, they were left untreated or were treated with 5 mM glutamate for 12 h. After treatment with glutamate, cells were harvested using 0.05% trypsin-EDTA. The collected cells were washed with phosphate-buffered saline (PBS; pH 7.4) and incubated with 2.5 μM DCF-DA, MitoSOX, and Fluo-4 AM for 20 min at 37°C. The cells then were washed with PBS twice and analyzed by flow cytometry (BD Bioscience, CA).

Annexin V and PI staining. The annexin V-fluorescein isothiocyanate (FITC)/PI apoptosis detection kit (BD Bioscience) was used to detect apoptosis by flow cytometry. The staining was conducted according to the manufacturer's instructions. After glutamate treatment, cells were collected and washed with PBS. Annexin V (5 μl) and PI (5 μl) next were added to the cell suspensions, and cells were incubated for 10 min at 37°C in the dark. They were then analyzed by flow cytometry.

Protein extraction and Western blot analysis. Proteins were extracted from cells using the PRO-PREP protein extraction solution (Intron Biotechnology, Seongnam, South Korea). Proteins were separated by 12% SDS-PAGE and then transferred onto nitrocellulose membranes (Pall, FL). Membranes were incubated with antibodies against Drp1 (catalog number sc-32898), Mfn1 (number sc-50330), and Mfn2 (number sc-50331) (Santa Cruz, CA); phosphorylated Drp1 (p-Drp1) (Ser 637) (number 4897S), cleaved caspase-3 (number 9661s), and calcineurin (number 2614S) (Cell Signaling, Danvers, MA); and peroxiredoxin 1 (Prx1) (number LA-PA0095), Prx2 (number LF-MA0144), Prx3 (number LF-MA0329), Prx4 (number LF-PA0009), Prx5 (number LF-PA0210), Prx6 (number LF-MA0018), and β-actin (number LF-PA0207) (Abfrontier, South Korea). We used horseradish peroxidase-conjugated anti-mouse and anti-rabbit IgGs (Thermo Scientific) as secondary antibodies. Protein bands were visualized with the Clarity Western ECL substrate (Bio-Rad, CA), and band intensities were analyzed with Multi Gauge, version 3.0, software (Fujifilm, Japan).

Mitochondrial imaging and analysis. DsRed2-mito-expressing HT22 cells were seeded on a poly-D-lysine-coated glass. The cells were then treated with glutamate for 12 h. Subsequently, the cells were fixed with 4% paraformaldehyde (Sigma-Aldrich). Images of the cells were acquired with an LSM-710 confocal microscope (Carl Zeiss, Jena, Germany), and the mitochondrial length was measured with ImageJ software (NIH, Bethesda, MD). The mitochondrial length was randomly measured, as previously described, from more than 50 mitochondrial particles per cell in more than 20 cells (63).

Statistical analysis. All experiments were repeated at least three times. Quantitative data are presented as the means ± standard deviations (SD) for the replicates. Data were analyzed by using analysis of variance on Prism 5.01 software (GraphPad Software Incorporated, CA). *P* values lower than 0.05 were considered statistically significant.

ACKNOWLEDGMENTS

M.H.K. and D.-S.L. performed the experiments and wrote the paper. H.J.L., S.-R.L., H.-S.L., J.-W.H., and Y.C.B. designed the study and experiments.

This research was supported by National Research Foundation of Korea (NRF) grants funded by the Korea government (NRF-2015R1A4A1042271, NRF-2017R1A2B4008176 and MSIT, and NRF-2017R1A5A2015391) and the KRIBB Research Initiative Program (KGM4621922).

We have no conflicts of interest to declare.

REFERENCES

1. Zhou Y, Danbolt NC. 2014. Glutamate as a neurotransmitter in the healthy brain. J Neural Transm (Vienna) 121:799–817. https://doi.org/10.1007/s00702-014-1180-8.
2. Choi DW. 1988. Glutamate neurotoxicity and diseases of the nervous system. Neuron 1:623–634. https://doi.org/10.1016/0896-6273(88)90162-6.
3. Lau A, Tymianski M. 2010. Glutamate receptors, neurotoxicity and neurodegeneration. Pflugers Arch 460:525–542. https://doi.org/10.1007/s00424-010-0809-1.
4. Mehta A, Prabhakar M, Kumar P, Deshmukh R, Sharma PL. 2013. Excitotoxicity: bridge to various triggers in neurodegenerative disorders. Eur J Pharmacol 698:6–18. https://doi.org/10.1016/j.ejphar.2012.10.032.
5. Meador-Woodruff JH, Healy DJ. 2000. Glutamate receptor expression in schizophrenic brain. Brain Res Brain Res Rev 31:288–294. https://doi.org/10.1016/S0165-0173(99)00044-2.
6. Lin X, Zhao Y, Li S. 2017. Astaxanthin attenuates glutamate-induced apoptosis via inhibition of calcium influx and endoplasmic reticulum stress. Eur J Pharmacol 806:43–51. https://doi.org/10.1016/j.ejphar.2017.04.008.
7. Tymianski M. 1996. Cytosolic calcium concentrations and cell death in vitro. Adv Neurol 71:85–105.
8. Arundine M, Tymianski M. 2004. Molecular mechanisms of glutamate-dependent neurodegeneration in ischemia and traumatic brain injury. Cell Mol Life Sci 61:657–668. https://doi.org/10.1007/s00018-003-3319-x.
9. Robinson BH. 1998. Human complex I deficiency: clinical spectrum and involvement of oxygen free radicals in the pathogenicity of the defect. Biochim Biophys Acta 1364:271–286. https://doi.org/10.1016/s0005-2728(98)00033-4.
10. Fleury C, Mignotte B, Vayssiere JL. 2002. Mitochondrial reactive oxygen species in cell death signaling. Biochimie 84:131–141. https://doi.org/10.1016/S0300-9084(02)01369-X.
11. Le Bras M, Clement MV, Pervaiz S, Brenner C. 2005. Reactive oxygen species and the mitochondrial signaling pathway of cell death. Histol Histopathol 20:205–219. https://doi.org/10.14670/HH-20.205.
12. Zhang Y, Lu X, Bhavnani BR. 2003. Equine estrogens differentially inhibit DNA fragmentation induced by glutamate in neuronal cells by modulation of regulatory proteins involved in programmed cell death. BMC Neurosci 4:32. https://doi.org/10.1186/1471-2202-4-32.
13. Ha JS, Park SS. 2006. Glutamate-induced oxidative stress, but not cell death, is largely dependent upon extracellular calcium in mouse neuronal HT22 cells. Neurosci Lett 393:165–169. https://doi.org/10.1016/j.neulet.2005.09.056.
14. Sattler R, Tymianski M. 2001. Molecular mechanisms of glutamate receptor-mediated excitotoxic neuronal cell death. Mol Neurobiol 24:107–129. https://doi.org/10.1385/MN:24:1-3:107.
15. Poynton RA, Hampton MB. 2014. Peroxiredoxins as biomarkers of oxidative stress. Biochim Biophys Acta 1840:906–912. https://doi.org/10.1016/j.bbagen.2013.08.001.
16. Lee DG, Kam MK, Kim KM, Kim HS, Kwon OS, Lee HS, Lee DS. 2018. Peroxiredoxin 5 prevents iron overload-induced neuronal death by inhibiting mitochondrial fragmentation and endoplasmic reticulum stress in mouse hippocampal HT-22 cells. Int J Biochem Cell Biol 102:10–19. https://doi.org/10.1016/j.biocel.2018.06.005.
17. Kim MH, Park SJ, Kim JH, Seong JB, Kim KM, Woo HA, Lee DS. 2018. Peroxiredoxin 5 regulates adipogenesis-attenuating oxidative stress in obese mouse models induced by a high-fat diet. Free Radic Biol Med 123:27–38. https://doi.org/10.1016/j.freeradbiomed.2018.05.061.
18. Park J, Kim B, Chae U, Lee DG, Kam MK, Lee SR, Lee S, Lee HS, Park JW, Lee DS. 2017. Peroxiredoxin 5 decreases beta-amyloid-mediated cyclin-dependent kinase 5 activation through regulation of Ca(2+)-mediated calpain activation. Antioxid Redox Signal 27:715–726. https://doi.org/10.1089/ars.2016.6810.
19. Park J, Choi H, Kim B, Chae U, Lee DG, Lee SR, Lee S, Lee HS, Lee DS. 2016. Peroxiredoxin 5 (Prx5) decreases LPS-induced microglial activation through regulation of Ca(2+)/calcineurin-Drp1-dependent mitochondrial fission. Free Radic Biol Med 99:392–404. https://doi.org/10.1016/j.freeradbiomed.2016.08.030.
20. Jin MH, Lee YH, Kim JM, Sun HN, Moon EY, Shong MH, Kim SU, Lee SH, Lee TH, Yu DY, Lee DS. 2005. Characterization of neural cell types expressing peroxiredoxins in mouse brain. Neurosci Lett 381:252–257. https://doi.org/10.1016/j.neulet.2005.02.048.
21. Cassano T, Pace L, Bedse G, Lavecchia AM, De Marco F, Gaetani S, Serviddio G. 2016. Glutamate and mitochondria: two prominent players in the oxidative stress-induced neurodegeneration. Curr Alzheimer Res 13:185–197. https://doi.org/10.2174/1567205013666151218132725.
22. Nunnari J, Marshall WF, Straight A, Murray A, Sedat JW, Walter P. 1997. Mitochondrial transmission during mating in Saccharomyces cerevisiae is determined by mitochondrial fusion and fission and the intramitochondrial segregation of mitochondrial DNA. Mol Biol Cell 8:1233–1242. https://doi.org/10.1091/mbc.8.7.1233.
23. Archer SL. 2013. Mitochondrial dynamics–mitochondrial fission and fusion in human diseases. N Engl J Med 369:2236–2251. https://doi.org/10.1056/NEJMra1215233.
24. Manczak M, Calkins MJ, Reddy PH. 2011. Impaired mitochondrial dynamics and abnormal interaction of amyloid beta with mitochondrial protein Drp1 in neurons from patients with Alzheimer's disease: implications for neuronal damage. Hum Mol Genet 20:2495–2509. https://doi.org/10.1093/hmg/ddr139.
25. Roe AJ, Qi X. 2018. Drp1 phosphorylation by MAPK1 causes mitochondrial dysfunction in cell culture model of Huntington's disease. Biochem Biophys Res Commun. https://doi.org/10.1016/j.bbrc.2018.01.114.
26. Hu C, Huang Y, Li L. 2017. Drp1-dependent mitochondrial fission plays critical roles in physiological and pathological progresses in mammals. Int J Mol Sci 18:E144. https://doi.org/10.3390/ijms18010144.
27. Chang CR, Blackstone C. 2007. Drp1 phosphorylation and mitochondrial regulation. EMBO Rep 8:1088–1089. https://doi.org/10.1038/sj.embor.7401118.
28. Jahani-Asl A, Slack RS. 2007. The phosphorylation state of Drp1 determines cell fate. EMBO Rep 8:912–913. https://doi.org/10.1038/sj.embor.7401077.
29. Cho B, Choi SY, Cho HM, Kim HJ, Sun W. 2013. Physiological and pathological significance of dynamin-related protein 1 (drp1)-dependent mitochondrial fission in the nervous system. Exp Neurobiol 22:149–157. https://doi.org/10.5607/en.2013.22.3.149.
30. Cereghetti GM, Stangherlin A, Martins de Brito O, Chang CR, Blackstone C, Bernardi P, Scorrano L. 2008. Dephosphorylation by calcineurin regulates translocation of Drp1 to mitochondria. Proc Natl Acad Sci U S A 105:15803–15808. https://doi.org/10.1073/pnas.0808249105.
31. Han XJ, Lu YF, Li SA, Kaitsuka T, Sato Y, Tomizawa K, Nairn AC, Takei K,

Matsui H, Matsushita M. 2008. CaM kinase I alpha-induced phosphorylation of Drp1 regulates mitochondrial morphology. J Cell Biol 182:573–585. https://doi.org/10.1083/jcb.200802164.
32. Meldrum BS. 2000. Glutamate as a neurotransmitter in the brain: review of physiology and pathology. J Nutr 130:1007S–1015S. https://doi.org/10.1093/jn/130.4.1007S.
33. Chan DC. 2006. Mitochondria: dynamic organelles in disease, aging, and development. Cell 125:1241–1252. https://doi.org/10.1016/j.cell.2006.06.010.
34. Musson RE, Smit NP. 2011. Regulatory mechanisms of calcineurin phosphatase activity. Curr Med Chem 18:301–315. https://doi.org/10.2174/092986711794088407.
35. Rhee SG, Kil IS. 2017. Multiple functions and regulation of mammalian peroxiredoxins. Annu Rev Biochem 86:749–775. https://doi.org/10.1146/annurev-biochem-060815-014431.
36. Kang SW, Rhee SG, Chang TS, Jeong W, Choi MH. 2005. 2-Cys peroxiredoxin function in intracellular signal transduction: therapeutic implications. Trends Mol Med 11:571–578. https://doi.org/10.1016/j.molmed.2005.10.006.
37. Shuvaeva TM, Novoselov VI, Fesenko EE, Lipkin VM. 2009. Peroxiredoxins, a new family of antioxidant proteins. Bioorg Khim 35:581–596.
38. Perkins A, Nelson KJ, Parsonage D, Poole LB, Karplus PA. 2015. Peroxiredoxins: guardians against oxidative stress and modulators of peroxide signaling. Trends Biochem Sci 40:435–445. https://doi.org/10.1016/j.tibs.2015.05.001.
39. Immenschuh S, Baumgart-Vogt E. 2005. Peroxiredoxins, oxidative stress, and cell proliferation. Antioxid Redox Signal 7:768–777. https://doi.org/10.1089/ars.2005.7.768.
40. Hudson AL, Sotirchos IM, Davey MW. 2011. The activity and hydrogen peroxide sensitivity of the peroxiredoxins from the parasitic nematode Haemonchus contortus. Mol Biochem Parasitol 176:17–24. https://doi.org/10.1016/j.molbiopara.2010.11.006.
41. Ahn HM, Yoo JW, Lee S, Lee HJ, Lee HS, Lee DS. 2017. Peroxiredoxin 5 promotes the epithelial-mesenchymal transition in colon cancer. Biochem Biophys Res Commun 487:580–586. https://doi.org/10.1016/j.bbrc.2017.04.094.
42. Radyuk SN, Michalak K, Klichko VI, Benes J, Orr WC. 2010. Peroxiredoxin 5 modulates immune response in Drosophila. Biochim Biophys Acta 1800:1153–1163. https://doi.org/10.1016/j.bbagen.2010.06.010.
43. Goemaere J, Knoops B. 2012. Peroxiredoxin distribution in the mouse brain with emphasis on neuronal populations affected in neurodegenerative disorders. J Comp Neurol 520:258–280. https://doi.org/10.1002/cne.22689.
44. Suzuki M, Nelson AD, Eickstaedt JB, Wallace K, Wright LS, Svendsen CN. 2006. Glutamate enhances proliferation and neurogenesis in human neural progenitor cell cultures derived from the fetal cortex. Eur J Neurosci 24:645–653. https://doi.org/10.1111/j.1460-9568.2006.04957.x.
45. Bruijn LI, Miller TM, Cleveland DW. 2004. Unraveling the mechanisms involved in motor neuron degeneration in ALS. Annu Rev Neurosci 27:723–749. https://doi.org/10.1146/annurev.neuro.27.070203.144244.
46. Caudle WM, Zhang J. 2009. Glutamate, excitotoxicity, and programmed cell death in Parkinson disease. Exp Neurol 220:230–233. https://doi.org/10.1016/j.expneurol.2009.09.027.
47. Coyle JT, Puttfarcken P. 1993. Oxidative stress, glutamate, and neurodegenerative disorders. Science 262:689–695. https://doi.org/10.1126/science.7901908.
48. Murphy TH, Miyamoto M, Sastre A, Schnaar RL, Coyle JT. 1989. Glutamate toxicity in a neuronal cell line involves inhibition of cystine transport leading to oxidative stress. Neuron 2:1547–1558. https://doi.org/10.1016/0896-6273(89)90043-3.
49. Kritis AA, Stamoula EG, Paniskaki KA, Vavilis TD. 2015. Researching glutamate-induced cytotoxicity in different cell lines: a comparative/collective analysis/study. Front Cell Neurosci 9:91. https://doi.org/10.3389/fncel.2015.00091.
50. Atlante A, Calissano P, Bobba A, Giannattasio S, Marra E, Passarella S. 2001. Glutamate neurotoxicity, oxidative stress and mitochondria. FEBS Lett 497:1–5. https://doi.org/10.1016/s0014-5793(01)02437-1.
51. Boulos S, Meloni BP, Arthur PG, Bojarski C, Knuckey NW. 2007. Peroxiredoxin 2 overexpression protects cortical neuronal cultures from ischemic and oxidative injury but not glutamate excitotoxicity, whereas Cu/Zn superoxide dismutase 1 overexpression protects only against oxidative injury. J Neurosci Res 85:3089–3097. https://doi.org/10.1002/jnr.21429.
52. Jia J, Zhang L, Shi X, Wu M, Zhou X, Liu X, Huo T. 2016. SOD2 mediates amifostine-induced protection against glutamate in PC12 cells. Oxid Med Cell Longev 2016:4202437. https://doi.org/10.1155/2016/4202437.
53. Fatma N, Kubo E, Sen M, Agarwal N, Thoreson WB, Camras CB, Singh DP. 2008. Peroxiredoxin 6 delivery attenuates TNF-alpha-and glutamate-induced retinal ganglion cell death by limiting ROS levels and maintaining Ca2+ homeostasis. Brain Res 1233:63–78. https://doi.org/10.1016/j.brainres.2008.07.076.
54. Yan Y, Wei CL, Zhang WR, Cheng HP, Liu J. 2006. Cross-talk between calcium and reactive oxygen species signaling. Acta Pharmacol Sin 27:821–826. https://doi.org/10.1111/j.1745-7254.2006.00390.x.
55. Kann O, Kovacs R. 2007. Mitochondria and neuronal activity. Am J Physiol Cell Physiol 292:C641–657. https://doi.org/10.1152/ajpcell.00222.2006.
56. Meeusen SL, Nunnari J. 2005. How mitochondria fuse. Curr Opin Cell Biol 17:389–394. https://doi.org/10.1016/j.ceb.2005.06.014.
57. Ni HM, Williams JA, Ding WX. 2015. Mitochondrial dynamics and mitochondrial quality control. Redox Biol 4:6–13. https://doi.org/10.1016/j.redox.2014.11.006.
58. Tilokani L, Nagashima S, Paupe V, Prudent J. 2018. Mitochondrial dynamics: overview of molecular mechanisms. Essays Biochem 62:341–360. https://doi.org/10.1042/EBC20170104.
59. Cribbs JT, Strack S. 2007. Reversible phosphorylation of Drp1 by cyclic AMP-dependent protein kinase and calcineurin regulates mitochondrial fission and cell death. EMBO Rep 8:939–944. https://doi.org/10.1038/sj.embor.7401062.
60. Southern JA, Young DF, Heaney F, Baumgartner WK, Randall RE. 1991. Identification of an epitope on the P and V proteins of simian virus 5 that distinguishes between two isolates with different biological characteristics. J Gen Virol 72:1551–1557. https://doi.org/10.1099/0022-1317-72-7-1551.
61. Knoops B, Goemaere J, Van der Eecken V, Declercq JP. 2011. Peroxiredoxin 5: structure, mechanism, and function of the mammalian atypical 2-Cys peroxiredoxin. Antioxid Redox Signal 15:817–829. https://doi.org/10.1089/ars.2010.3584.
62. Kim B, Park J, Chang KT, Lee DS. 2016. Peroxiredoxin 5 prevents amyloid-beta oligomer-induced neuronal cell death by inhibiting ERK-Drp1-mediated mitochondrial fragmentation. Free Radic Biol Med 90:184–194. https://doi.org/10.1016/j.freeradbiomed.2015.11.015.
63. Park J, Choi H, Min JS, Park SJ, Kim JH, Park HJ, Kim B, Chae JI, Yim M, Lee DS. 2013. Mitochondrial dynamics modulate the expression of pro-inflammatory mediators in microglial cells. J Neurochem 127:221–232. https://doi.org/10.1111/jnc.12361.